High-Pressure Phase Behavior of Eight Binary Mixtures of Pyrimidine or Pyrazine with CO_2, C_2H_4, C_2H_6, or CHF_3

Seiichi Yamamoto, Kazunari Ohgaki,* and Takashi Katayama*

Department of Chemical Engineering, Faculty of Engineering Science, Osaka University, Toyonaka, Osaka 560, Japan

High-pressure phase behavior for eight binary mixtures consisting of pyrimidine or pyrazine with CO_2, C_2H_4, C_2H_6, or CHF_3 is investigated in the temperature range from 210 to 340 K and pressures up to 30 MPa. The observed phase boundaries correspond to gas-liquid critical lines and three-phase coexistence lines, including critical end points and quadruple points. The pressure-temperature-gaseous phase composition relations are given along the boundaries that are determined by straightforward visual observation through an equilibrium view cell. The gaseous phase composition is obtained by use of supercritical fluid chromatography. The transitional patterns of pressure-temperature diagrams are briefly discussed in terms of the characteristic interactions and the magnitudes of size asymmetry between unlike molecules.

Introduction

The phase behavior of a homologous series of binary mixtures has been examined by several investigators, since it is fundamental information for the design and operation of industrial processes. The series that have been reported include the CH_4 + *n*-alkane series, the C_2H_6 + *n*-alkane series, the CO_2 + *n*-alkane series, the C_2H_6 + *n*-alkylbenzene series, and the CO_2 + *n*-alkylbenzene series (*1-5*). The phase behavior of binary mixtures having a supercritical component has also been studied by McHugh and Yogan (*6*) and Cheong et al. (*7*) from the standpoint of utilizing supercritical fluids for new processes. Recently, Luks (*1*) has summarized systematic evolution in the phase behavior of binary mixtures by use of six typical types of phase diagrams in terms of asymmetry between unlike molecules. Experimental determination of phase behavior for such mixtures still continues to be of importance, owing to the lack of sound theoretical relationships.

In a previous study (*8*), the phase behavior for eight binary mixtures of indole or quinoxaline with CO_2, C_2H_4, C_2H_6, or CHF_3 was investigated around the critical point of the light component. Also, we tried to summarize types of phase diagrams in terms of the temperature difference between the melting temperature of the heavy component and the critical temperature of the light component. At that time, we could not determine that the quinoxaline + CO_2 system belongs to type "B" of Luks' classification shown in Figure 1, since the data in the low-temperature region (around the triple point of CO_2) was lacking.

One of the aims of the present study is to clarify the high-pressure phase boundaries in a wide temperature range. Pressure-temperature-gaseous phase composition relations are determined for the observed phase boundaries, which include a gas-liquid critical line (G=L), three-phase coexistence lines (S-L-L, S-L-G, L-L-G), and their terminals (critical end points and quadruple points). Here, G represents gaseous phase, L liquid phase, and S solid phase. The light components investigated are CO_2, C_2H_4, C_2H_6, and CHF_3 whose critical temperatures are 304.1, 282.4, 305.4, and 299.3 K, respectively. The heavy components investigated are two isomers, that is, pyrimidine (1,3-diazine) and pyrazine (1,4-diazine). The normal melting temperature of pyrazine (324.3 K) is higher than the critical temperature of any light component, while that of pyrimidine (293.0 K) lies between the critical temperatures of C_2H_4 and of CHF_3.

Experimental Section

Measurement around the Critical Temperature of the Light Component. The experimental apparatus consists of a phase equilibrium part and a supercritical fluid chromatograph (SFC) part. A detailed description of the experimental apparatus and the procedure is given in a previous paper (*8*).

A binary mixture under investigation was confined in a constant volume view cell (ca. 100 cm^3) of the phase equilibrium part. The cell can stand pressures up to 30 MPa. Then the mixture in the cell was agitated well by a magnetic stirrer to establish equilibrium. In order to obtain the phase boundaries, the temperature of a water bath surrounding the cell was changed or the pressure in the cell was isothermally raised by supplying the light component. The phase boundaries were determined by straightforward visual observation. When a phase boundary appeared, the pressure in the cell and the temperature of the water bath were measured, and the concentration of the gaseous phase was determined by injecting a small amount of the phase (ca. 0.0012 cm^3) into the SFC. A detailed description of the sampling procedure (a direct injection method into the SFC without a pressure drop) and the calibration method are given in an earlier paper (*9*).

The equilibrium pressure was measured with a pressure transducer to an accuracy of ±0.065 MPa, and the temperature was measured to ±0.01 K with a digital temperature sensor. Although the temperature sensor was set just outside of the cell, it indicated the same temperature in the cell since the temperature of the water bath was kept constant or changed very gradually (ca. 0.3 K/h), according to the kind of phase boundaries.

Measurement in the Low-Temperature Region. When there was a possibility of existence of a liquid-liquid immiscibility in the temperature range lower than 0 °C, a supplementary experiment was performed by use of another apparatus. In this case, two cells, a glass cell (ca. 20 cm^3) and a semitransparent-tube cell (ca. 5 cm^3, $^1/_4$-in. o.d.), were used for pressure ranges up to 1.5 and 3 MPa, respectively. Several stainless balls (6.2 mm) or glass balls (3.7 mm) were put in the cells to agitate a binary mixture by shaking.

The procedure was as follows. A proper amount of a heavy component was charged in one of the cells. Then the sample was outgassed under vacuum for several minutes at room temperature prior to supply of a light component. After that, the cell was cooled to about 230 K in an ethanol + dry ice bath. The light component was supplied into the cell and condensed so as to establish a three-phase S-L-G equilibrium that lay slightly under the vapor-pressure curve of the pure light component. In order to ascertain whether the liquid-liquid immiscibility occurs or not, visual observation was performed along the S-L-G equilibrium condition with a temperature swing. When the immiscibility is present, the solid phase starts to melt with a rise in temperature, resulting in the appearance of another liquid phase, that is, the four-phase S-L-L-G equilibrium. However, when the immiscibility is absent, no phase transition

0021-9568/90/1735-0310$02.50/0

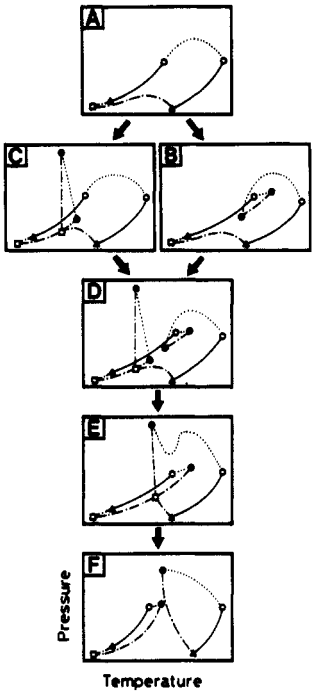

Figure 1. Six types of phase behavior for binary mixtures shown as pressure–temperature projections: (○) critical point, (△) triple point, (●) critical end point, (□) quadruple point, (—) two-phase line, (···) critical line, (– · –) three-phase line.

Table I. Experimental Pressure–Temperature–Gaseous Phase Composition Data of the Phase Boundaries for the Pyrimidine (1) + CO_2 (2) System (Type A)

p/MPa	T/K	y_1
	S_1–L–G	
0.89	285.21	
1.42	277.78	
	G=L	
7.86	308.39	0.00539
8.31	313.01	0.0146
8.82	318.01	0.0251
9.83	326.91	0.0455
10.65	332.62	0.0573
	From the Supplementary Experiment[a]	
	S_1–L–G	
1.61	270.0	
1.58	260.0	
1.35	250.0	
1.09	240.0	
0.87	230.0	
0.59	220.0	
	S_1–S_2–L–G	
0.43	209.9	

[a] Data obtained by the apparatus for the low-temperature condition.

occurs, and consequently the S–L–G coexistence curve starts to deviate from the vapor-pressure curve of the pure light component and finally terminates at the triple point of the pure heavy component. The three-phase S–L–G pressures were measured at temperatures of regular intervals; however, the gaseous phase compositions were not analyzed since the phase was almost pure.

The equilibrium pressure was measured with a pressure gauge to an accuracy of ±1% and the temperature with an alcohol thermometer to ±0.2 K in the low-temperature experiment.

Materials. Both pyrimidine (Aldrich, 99%) and pyrazine (Aldrich, 99%) were used as received. Carbon dioxide was purchased from Takachiho Kagakukogyo K. K., having a stated minimum purity of 99.9%. Both ethylene and ethane were provided by Nippon Fine Gas Co. with certified minimum purities of 99.97% and 99.6%, respectively. Trifluoromethane was provided by Daikin Industries, Ltd. with a certified minimum purity of 99.999%. All gases were used without further purification.

Table II. Experimental Pressure–Temperature–Gaseous Phase Composition Data of the Phase Boundaries for the Pyrazine (1) + CO_2 (2) System (Type A)

p/MPa	T/K	y_1
	S_1–L–G	
0.89	319.62	
2.08	310.00	0.00181
2.75	301.54	0.00320
2.99	290.02	0.00273
2.67	277.30	0.00141
	G=L	
8.25	313.72	0.0181
9.56	326.25	0.0441
10.54	333.57	0.0526
	From the Supplementary Experiment[a]	
	S_1–L–G	
2.44	270.0	
2.05	260.0	
1.60	250.0	
1.17	240.0	
0.82	230.0	
0.61	220.0	
	S_1–S_2–L–G	
0.45	212.2	

[a] Data obtained by the apparatus for the low-temperature condition.

Table III. Experimental Pressure–Temperature–Gaseous Phase Composition Data of the Phase Boundaries for the Pyrimidine (1) + CHF_3 (2) System (Type A)

p/MPa	T/K	y_1
	S_1–L–G	
0.96	286.49	
1.40	279.48	
	G=L	
4.98	301.73	0.00646
5.20	304.69	0.0132
5.49	308.60	0.0222
5.79	313.15	0.0350
6.08	317.87	0.0446
6.60	325.47	0.0651
	From the Supplementary Experiment[a]	
	S_1–L–G	
1.45	270.0	
1.29	260.0	
1.02	250.0	
0.78	240.0	
0.59	230.0	

[a] Data obtained by the apparatus for the low-temperature condition.

Results and Discussion

Tables I–VIII give the experimental pressure–temperature–gaseous phase composition (p–T–y_1) relations of the phase boundaries for the eight systems investigated. The gas–liquid critical point is represented as "G=L", the three-phase coexistence equilibria as "S_1–L–G", etc., the quadruple points as "S_1–S_2–L–G", etc., and the critical end points where gaseous phase and liquid phase are critically identical in the presence of another phase as "S_1–L=G", etc. The symbols S_1 and S_2

Table IV. Experimental Pressure–Temperature–Gaseous Phase Composition Data of the Phase Boundaries for the Pyrazine (1) + CHF_3 (2) System (Type A)

p/MPa	T/K	y_1
	S_1–L–G	
1.03	320.82	
2.09	314.98	0.004 98
2.65	309.93	0.006 17
3.02	302.00	0.005 68
2.86	291.35	0.003 99
2.31	277.79	0.003 12
	G=L	
5.69	312.15	0.033 5
6.16	318.59	0.045 5
6.80	327.15	0.057 1
	From the Supplementary Experiment[a]	
	S_1–L–G	
2.00	270.0	
1.57	260.0	
1.15	250.0	
0.84	240.0	
0.61	230.0	
0.43	220.0	

[a] Data obtained by the apparatus for the low-temperature condition.

Table V. Experimental Pressure–Temperature–Gaseous Phase Composition Data of the Phase Boundaries for the Pyrimidine (1) + C_2H_6 (2) System (Type E)

p/MPa	T/K	y_1
	S_1–L–G	
1.21	290.45	
2.37	288.02	
	S_1–L_1–L_2–G	
3.01	286.20	0.003 50
	S_1–L_1–L_2	
5.61	286.61	0.028 9
9.45	287.00	0.033 1
13.16	287.92	0.038 1
20.12	288.69	0.043 1
27.36	289.77	0.049 2
	S_1–L–G	
2.57	278.00	0.002 68
2.80	282.00	0.003 03
	L_1–L_2–G	
3.43	292.00	0.004 51
3.85	298.00	0.005 03
4.38	304.00	0.006 38
4.89	309.00	0.008 41
	L_1–L_2=G	
5.33	313.90	0.014 3

stand for the solid phases of the pure heavy component and the pure light component, respectively. Also the symbol L_1 is chosen to represent a liquid phase where the mole fraction of the heavy component is larger than that of the other liquid phase, L_2, in equilibrium. For the S_1–L_1–L_2 equilibrium, the L_2 phase was sampled and the concentration of the phase was determined. The uncertainty in mole fraction, ±2%, corresponded to the uncertainty in the SFC analysis, and the temperatures were reproducible to ±0.05 K on repeated runs.

The eight systems were found to be classified into three types of phase behavior. Figure 1 shows the six principal phase diagrams for binary mixtures in conformity with those of Luks (*1*), who gave attention to evolution of the three-phase L–L–G coexistence lines. The components are restricted to nonpolar or moderately polar nonelectrolyte. The classification is somewhat different from those of Rowlinson and Swinton (*5*) and van Konynenburg and Scott (*10*), since treatment of the

Table VI. Experimental Pressure–Temperature–Gaseous Phase Composition Data of the Phase Boundaries for the Pyrazine (1) + C_2H_6 (2) System (Type E)

p/MPa	T/K	y_1
	S_1–L–G	
1.06	322.82	
2.11	320.51	
3.95	316.32	0.008 00
	S_1–L_1–L_2–G	
5.19	313.49	0.011 5
	S_1–L_1–L_2	
6.98	313.40	0.043 3
10.09	313.45	0.048 7
13.33	313.71	0.052 9
16.56	313.78	0.057 2
20.72	314.21	0.061 6
	S_1–L–G	
4.43	303.00	0.003 99
4.71	307.00	0.005 94
5.04	311.00	0.008 51
	L_1–L_2–G	
5.38	315.00	0.013 2
5.56	317.00	0.017 3
	L_1–L_2=G	
5.71	318.67	0.024 0

Table VII. Experimental Pressure–Temperature–Gaseous Phase Composition Data of the Phase Boundaries for the Pyrimidine (1) + C_2H_4 (2) System (Type E)

p/MPa	T/K	y_1
	S_1–L–G	
1.33	289.59	
2.20	286.94	
3.54	283.03	0.002 45
	S_1–L_1–L_2–G	
4.51	279.51	0.002 33
	S_1–L_1–L_2	
6.02	279.46	0.044 1
9.47	279.17	0.058 3
14.06	279.03	0.069 5
	S_1–L–G	
4.18	276.00	0.001 80
	L_1–L_2–G	
4.90	284.00	0.003 71
5.33	288.00	0.005 90
	L_1–L_2=G	
5.80	291.97	0.018 4

solid phase was not considered in those articles. With increasing asymmetry between unlike molecules, the phase behavior evolves from type A to type F. The type of phase behavior for each mixture is also represented in Tables I–VIII according to the above categories.

The four systems were identified to belong to type A phase behavior. They are the pyrimidine + CO_2 and + CHF_3 and the pyrazine + CO_2 and + CHF_3 systems (Tables I–IV). For each of the above four systems, the supplementary experiment was performed in order to ascertain whether the liquid–liquid immiscibility occurs (type C) or not (type A) in the temperature range lower than 0 °C. For the two CO_2 systems, the other terminus of the S_1–L–G line was determined, when the liquid phase rich in CO_2 began to crystallize, as a quadruple point where four phases (S_1–S_2–L–G) coexisted in equilibrium. In other words, no liquid–liquid immiscibility was observed before the onset of crystallization. The pressure–temperature (p–T) trace of the phase boundaries for the pyrazine + CO_2 system is shown in Figure 2. The gas–liquid critical line commences at the critical point of pure CO_2 (304.1 K, 7.38 MPa) and ends

Table VIII. Experimental Pressure–Temperature–Gaseous Phase Composition Data of the Phase Boundaries for the Pyrazine (1) + C_2H_4 (2) System (Type F)

p/MPa	T/K	y_1
	S_1–L–G	
1.02	321.38	
2.11	319.03	
3.66	313.50	0.005 47
4.87	310.62	0.006 69
6.81	305.65	0.017 9
7.40	304.86	0.042 0
8.75	304.51	0.061 7
9.66	304.17	0.085 3
	G=L	
9.98	305.21	0.101
10.35	310.80	0.105
	S_1–L–G	
4.54	280.00	0.001 59
4.92	284.00	0.002 57
5.31	288.00	0.004 47
	S_1–L=G	
5.56	290.82	0.009 51

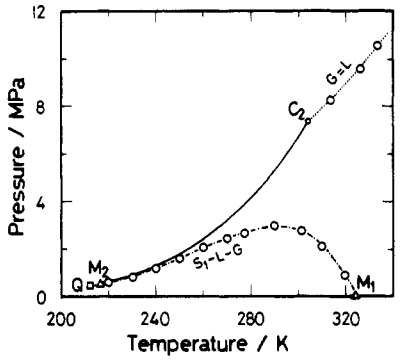

Figure 2. Pressure–temperature trace of the phase boundaries for the pyrazine + CO_2 system: (C_2) critical point of CO_2, (M_1) triple point of pyrazine, (M_2) triple point of CO_2, (Q) quadruple point of S_1–S_2–L–G, (—, between C_2 and M_2) vapor-pressure curve of CO_2.

at the critical point of pure pyrazine (622.0 K, 5.80 MPa) continuously through a pressure maximum. The three-phase S_1–L–G line starts at the triple point of pure pyrazine (324.3 K) and, through a pressure maximum, terminates at the quadruple point (212.2 K, 0.45 MPa). The temperature difference between the triple point of pure CO_2 (216.6 K, 0.52 MPa) and the quadruple point, that is, the freezing point depression of CO_2, is 4.4 K. This value is 6.7 K for the pyrimidine + CO_2 system. For the two CHF_3 systems, no liquid–liquid immiscibility also was observed between 220 and 273 K. Since the solubility of solid in liquid CHF_3 decreases with decreasing temperature, the binary three-phase S_1–L–G line nearly coincides with the vapor-pressure curve of pure CHF_3 at around 220 K, and consequently the liquid–liquid immiscibility is likely not to appear at lower temperatures.

In a previous paper (*8*), a liquid–liquid immiscibility was observed near the critical point of CO_2 for the quinoxaline + CO_2 system. However, because of lack of data in temperatures lower than 0 °C, it could not be determined whether another liquid–liquid immiscibility occurs (type D) or not (type B). The supplementary experiment was also performed for this system. Since any other liquid–liquid immiscibility was not observed before the onset of crystallization of CO_2 in the almost pure CO_2 liquid phase, the system was identified to belong to type B phase behavior. The freezing point depression of CO_2 is 3.9 K for the system.

The three systems were revealed to show type E phase behavior. They are the pyrimidine + C_2H_6 and + C_2H_4 and the pyrazine + C_2H_6 systems (Tables V–VII). The p–T trace of

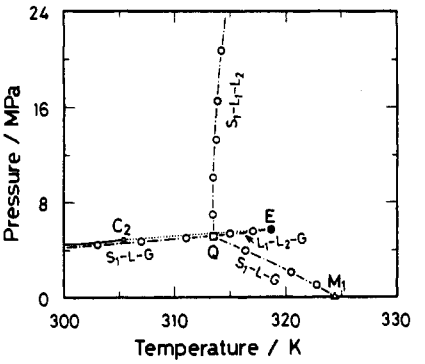

Figure 3. Pressure–temperature trace of the phase boundaries for the pyrazine + C_2H_6 system: (C_2) critical point of C_2H_6, (E) upper critical end point, (M_1) triple point of pyrazine, (Q) quadruple point of S_1–L_1–L_2–G.

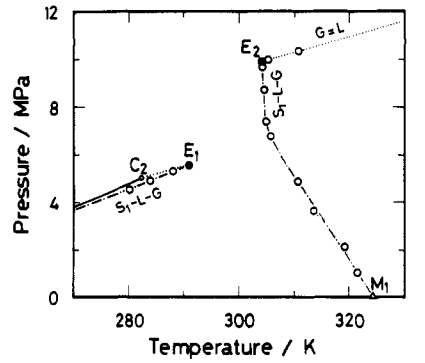

Figure 4. Pressure–temperature trace of the phase boundaries for the pyrazine + C_2H_4 system: (C_2) critical point of C_2H_4, (E_1) first critical end point, (E_2) second critical end point, (M_1) triple point of pyrazine.

the phase boundaries for the pyrazine + C_2H_6 system is shown in Figure 3. The four three-phase coexistence lines concentrate in a quadruple point where four phases (S_1–L_1–L_2–G) are in equilibrium. The characteristic feature of this system is that the quadruple point temperature (313.5 K) is higher than the critical temperature of the light component, C_2H_6 (305.4 K). The phase behavior of this system is undoubtedly type E but close to type F behavior. The quadruple point (S_1–L_1–L_2–G) temperatures of the pyrimidine + C_2H_6 and + C_2H_4 systems are lower than the critical temperatures of C_2H_6 and C_2H_4, respectively, as usual.

The phase behavior of the pyrazine + C_2H_4 system (Table VIII) belongs to type F, since the triple point temperature of pyrazine (324.3 K) and the critical temperature of C_2H_4 (282.4 K) are fairly separated. The p–T trace of the phase boundaries for the system is shown in Figure 4. The low-temperature branch of the S_1–L–G line terminates at the so-called first critical end point (S_1–L=G; 290.8 K, 5.56 MPa) where gaseous and liquid phases are critically identical in the presence of solid pyrazine. The high-temperature branch of the S_1–L–G line commences at the triple point of pyrazine and terminates at the so-called second critical end point (S_1–L=G). The gas–liquid critical line (G=L) connects the second critical end point and the critical point of pyrazine through a pressure maximum. The values of p, T, and y_1 at the second critical end point were evaluated to be 9.91 MPa, 304.1 K, and 0.10, respectively, by means of extrapolation, since it is experimentally difficult to reach the point exactly.

In the previous study (*8*), the relations of the type of phase diagram and the temperature difference $\Delta T (\equiv T_{m,1} - T_{c,2})$ were discussed, where $T_{m,1}$ is the melting temperature of the heavy component and $T_{c,2}$ is the critical temperature of the light component. When the ΔT value is larger than 20 K, the type of phase behavior is type F for the indole systems. In the

present study, both the pyrazine + CO_2 and + CHF_3 systems show type A phase behavior, in spite of large values of ΔT (both larger than 20 K). These findings would reflect some characteristic interactions between unlike molecules such as the strong affinity between CO_2 and Lewis base.

Conclusions

Pressure-temperature-gaseous phase composition relations of high-pressure phase boundaries are reported for eight binary mixtures, which are composed of pyrimidine or pyrazine as the heavy component and CO_2, C_2H_4, C_2H_6, or CHF_3 as the light component. The phase boundaries are determined by straightforward visual observation, and in order to determine the gaseous phase composition, a small amount of the phase (ca. 0.012 cm^3) is injected into the SFC. The observed phase boundaries are the gas-liquid critical line (G=L), the three-phase equilibrium lines (S_1-L_1-L_2, S_1-L-G, L_1-L_2-G), the critical end points (S_1-L=G, L_1-L_2=G), and the quadruple points (S_1-S_2-L-G, S_1-L_1-L_2-G).

The pyrimidine + CO_2 and + CHF_3 systems and the pyrazine + CO_2 and + CHF_3 systems are identified to show type A phase behavior according to the arbitrarily defined classification of phase behavior (Figure 1). The pyrimidine + C_2H_6 and + C_2H_4 systems and the pyrazine + C_2H_6 system are identified to display type E phase behavior. And the pyrazine + C_2H_4 system is revealed to belong to type F behavior. Although the ΔT values of both the pyrazine + CO_2 and + CHF_3 systems are large enough to show type F, both systems show type A.

Acknowledgment

We are grateful to Nippon Fine Gas Co. and Daikin Industries, Ltd., for supplying the sample gases. We are also grateful to Tsuyoshi Hagiwara for his experimental assistance.

Registry No. CO_2, 124-38-9; C_2H_4, 74-85-1; C_2H_6, 74-84-0; CHF_3, 75-46-7; pyrimidine, 289-95-2; pyrazine, 290-37-9.

Literature Cited

(1) Luks, K. D. *Fluid Phase Equillb.* **1986**, *29*, 209-224.
(2) Peters, C. J.; Lichtenthaler, R. N.; de Swaan Arons, J. *Fluid Phase Equilib.* **1986**, *29*, 495-504.
(3) Schneider, G. M. *Angew. Chem., Int. Ed. Engl.* **1978**, *17*, 716-727.
(4) Miller, M. M.; Luks, K. D. *Fluid Phase Equilib.* **1989**, *44*, 295-304.
(5) Rowlinson, J. S.; Swinton, F. L. *Liquids and Liquid Mixtures*, 3rd ed.; Butterworth: London, 1982; Chapter 6.
(6) McHugh, M. A.; Yogan, T. J. *J. Chem. Eng. Data* **1984**, *29*, 112-115.
(7) Cheong, P. L.; Zhang, D.; Ohgaki, K.; Lu, B. C.-Y. *Fluid Phase Equilib.* **1986**, *29*, 555-562.
(8) Yamamoto, S.; Ohgaki, K.; Katayama, T. *J. Supercrit. Fluids* **1989**, *2*, 63-72.
(9) Sako, S.; Ohgaki, K.; Katayama, T. *J. Supercrit. Fluids* **1988**, *1*, 1-6.
(10) van Konynenburg, P. H.; Scott, R. L. *Philos. Trans. R. Soc. London* **1980**, *A298*, 495-540.

Received for review October 30, 1989. Accepted March 23, 1990. This work was partly supported by a Grant-in-Aid for Scientific Research from the Ministry of Education, Science, and Culture of Japan.

Excess Second Virial Coefficients for Binary Mixtures of Carbon Dioxide with Methane, Ethane, and Propane

Peter J. McElroy,* Lim Leong Kee, and Craig A. Renner

Chemical and Process Engineering, University of Canterbury, Christchurch, New Zealand

For the binary systems methane + carbon dioxide, ethane + carbon dioxide, and propane + carbon dioxide, measurements of the pressure change on mixing at 303.15, 313.15 and 323.15 K are reported as well as the excess second virial coefficients calculated therefrom. The correlations due to Tsonopoulos, Hayden and O'Connell, and the Groupe Européen de Recherches Gazières are compared with the results.

Introduction

Apart from the virial equation, virtually all equations of state have been developed for single-component systems and extended to mixtures by application of combining rules for the parameters. These rules are invariably arbitrary in nature despite attempts to relate them to fundamental theory. The virial equation has the great advantage that the equations describing mixture behavior are rigorously derived from statistical mechanics.

At high pressures the virial equation has often been rejected because the series may not converge rapidly. In recent years, however, it has been demonstrated that for certain gas mixtures of industrial importance (e.g. reticulated natural gas), an excellent fit to available data can be obtained with second and third virial coefficients only (*1*). Consequently, the excellent features of the equation may be taken advantage of.

This study represents part of a broader investigation into both second and third virial coefficients.

The pressure change of mixing method used here employs relation 1 where y, P, ΔP, and T are respectively the mole fraction, the pressure, the pressure change, and the temperature. The method has the advantage over measuring the

$$RT\Delta P/[P^2(1 + \Delta P/P)2y(1 - y)] = B_{12} - (B_{11} + B_{22})/2 = B^E_{12} \quad (1)$$

second molar virial coefficient B_m of a mixture that it is possible to measure the second molar excess virial coefficient E^E_{12} with greater accuracy than the second molar virial coefficients B_{11} and B_{22} of the pure gases, so that determination of the unlike interaction second molar virial coefficient B_{12} to an accuracy comparable with that of B_{11} and B_{22} can be achieved.

Experimental Apparatus and Procedure

The apparatus, which has been described previously (*2*), consists essentially of three equally sized glass vessels, immersed in an oil bath. The first vessel contains gas maintained as a reference pressure, the second and third, components 1 and 2 all, at equal pressure. The two components are mixed and the resultant change in pressure is measured relative to the reference pressure.

The only change to the apparatus was the addition of two gas drying trains fitted with mercury-filled pressure relief "bubblers" with access tubes of sufficient height for the "train" to be evacuated prior to filling with test gas.

0021-9568/90/1735-0314$02.50/0